Response of FBGs in Microstructured and Bow Tie Fibers Embedded in Laminated Composite

Geert Luyckx, Eli Voet, Thomas Geernaert, Karima Chah, Tomasz Nasilowski, *Member, IEEE*, Wim De Waele, Wim Van Paepegem, Martin Becker, Hartmut Bartelt, Waclaw Urbanczyk, Jan Wojcik, Joris Degrieck, Francis Berghmans, *Member, IEEE*, and Hugo Thienpont, *Associate Member, IEEE*

***Abstract*—Fiber Bragg gratings in bow tie fiber and highly birefringent microstructured optical fiber are embedded in a carbon fiber reinforced epoxy. The Bragg peak wavelength shifts of the embedded gratings are measured under controlled bending, transversal loading, and thermal cycling of the composite sample. We obtain similar axial and transversal strain sensitivities for the two embedded fiber types. We also highlight the low temperature dependence of the Bragg peak separation of the microstructured fibers, which is an important advantage for this application. The results show the feasibility of using microstructured fibers in structural integrity monitoring.**

***Index Terms*—Gratings, optical fibers, strain measurement, temperature measurement.**

I. Introduction

SURFACE-MOUNTED axial strain measurement is one of the most important applications of fiber Bragg grating (FBG) based sensor technology [1]. However, to monitor the structural health of more complex materials such as fiber-reinforced plastics, it is necessary to map the internal strain field of the material, and more particularly, the transversal strain that can cause catastrophic damage, e.g., delamination. FBGs written in the conventional birefringent fiber (e.g., bow tie and panda fiber) are found adequate for this purpose [2]. The internal strain field can be measured almost straightforwardly whenever temperature is kept constant. *In situ* strain measurements, however, require a correction mechanism for the intrinsic temperature sensitivity of the Bragg grating sensors. Although the Bragg peaks of FBGs in classical birefringent fibers (bow tie, panda, elliptical cladding, ...) feature a small difference in temperature sensitivity [3], discriminating axial strain and temperature remains very difficult [2], [4]. Instead, one typically relies on an additional embedded sensor to correct for temperature variations that should be isolated from the existing strain field by encapsulating it with a (glass, fused silica, or metal) capillary [2], [5], [6]. The presence of a capillary can, however, disturb the structure of the material under test. Tanaka *et al.* [7] compensate for temperature via an FBG embedded in a surface-mounted composite plate on top of the structure. Most of the reports in literature address the cross-sensitivity of axial strain and temperature variations only, and omit the existing transverse strains while these are precisely interesting in terms of damage assessment.

In this letter, we solve both issues simultaneously by using FBGs in highly birefringent microstructured optical fibers (MOFs). Such fibers are well known to offer unprecedented design flexibility as their microstructure can possibly be tailored to and optimized for a particular application [8]. We previously demonstrated that FBGs in MOFs [9]–[13] can be successfully embedded in composite materials [14]. In this letter, we benchmark the capabilities of FBGs in MOFs against FBGs written in conventional birefringent optical fibers (bow tie). We embedded both types of sensors in a fiber-reinforced plastic (carbon–epoxy) coupon, and we compare the response of the fiber sensors when the composite material is exposed to controlled mechanical and thermal load. This allows assessing the real potential of FBGs in MOFs in structural health monitoring.

II. Embedded Optical Fiber Technology

The first FBG is written in an 80-μm cladding bow tie fiber from Fibercore, Inc. The birefringence in this fiber is induced by stress-applying parts in bow tie shape (boron-doped silica) in the fiber cladding. At 1550 nm, the phase modal birefringence in this fiber is 3×10^{-4}. The second grating is written in a 125-μm highly birefringent MOF (Fig. 1). The phase modal birefringence in this fiber mainly originates from the microstructure's geometry and was measured to be 8×10^{-4} at 1550 nm [14]. As depicted in Fig. 1, FBGs in a birefringent fiber yield two Bragg peaks ($\lambda_{\text{slow}}, \lambda_{\text{fast}}$), corresponding to both orthogonally polarized modes. Since the Bragg peak separation depends on the phase modal birefringence, the two Bragg peaks in the MOF are much more separated than in the bow tie FBG. This large wavelength separation facilitates the peak detection and allows

Manuscript received April 24, 2009; revised May 19, 2009. First published June 23, 2009; current version published September 02, 2009. This work was supported in part by the EU FP6 "Network of Excellence for Micro-Optics (NEMO)" Network, in part by the EU FP7 Project "Photonic Skins For Optical Sensing (PHOSFOS)," in part by the COST 299 Action "Optical Fibres for New Challenges Facing the Information Society (FIDES)," in part by the IWT SBO Project "Flexible Artificial Optical Skin (FAOS)," and in part by the Fund for Scientific Research, Flanders (FWO-Vlaanderen), Belgian Federal Interuniversity Poles of Attraction (IAP) and Flemish Concerted Research Actions (GOA). The work of T. Geernaert was supported by the Institute for the Promotion of Innovation through Science and Technology in Flanders (IWT-Vlaanderen).

G. Luyckx, E. Voet, W. De Waele, W. Van Paepegem, and J. Degrieck are with the Department of Materials Science and Engineering, Ghent University, 9000 Gent, Belgium (e-mail: geert.luyckx@ugent.be; eli.voet@ugent.be; wim.dewaele@ugent.be; wim.vanpaepegem@ugent.be; joris.degrieck@ugent.be).

T. Geernaert, K. Chah, T. Nasilowski, F. Berghmans, and H. Thienpont are with the Vrije Universiteit Brussel, 1050 Brussel, Belgium (e-mail: thomas.geernaert@vub.ac.be; kachah@tona.vub.ac.be; tnasilowski@tona.vub.ac.be; fberghma@vub.ac.be; hthienpo@vub.ac.be).

M. Becker and H. Bartelt are with the Institute of Photonic Technology, D-07745 Jena, Germany (e-mail: martin.becker@ipht-jena.de; hartmut.bartelt@ipht-jena.de).

W. Urbanczyk is with Wroclaw University of Technology, 50-370 Wroclaw, Poland (e-mail: waclaw.urbanczyk@pwr.wroc.pl).

J. Wojcik is with the Maria Curie-Sklodowska University, 20-031 Lublin, Poland (e-mail: jan.wojcik@umcs.lublin.pl).

Digital Object Identifier 10.1109/LPT.2009.2025262

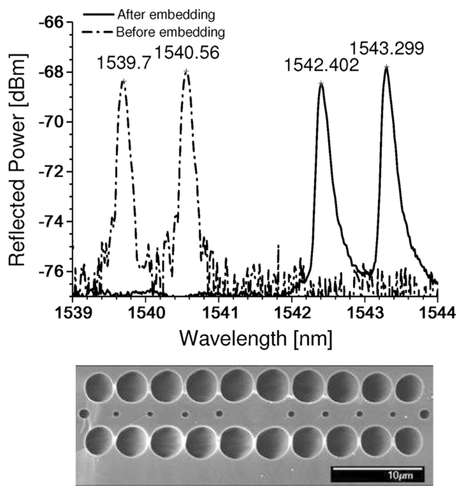

Fig. 1. (Top) Spectra of the FBG in the MOF before (dashed–dotted line) and after embedding (solid line). Due to residual strains in the composite structure (after curing), the peak separation has changed. (Bottom) Profile of the MOF fiber.

TABLE I
ORIENTATION OF THE EMBEDDED OPTICAL FIBERS

Orientation [°] (angle between slow axis and composite surface)	Bow tie	MOF
Sample 1	13	15
Sample 2	60	12

a more accurate measurement of the peak wavelengths. Third, we also used a grating in a conventional single-mode FBG (SM FBG) as a reference sensor.

The Bragg gratings have been embedded between the second and the third layers of a layup of 16 carbon fiber epoxy unidirectional prepreg layers with a total thickness of 1.54 mm (M18/M55J material from Hexcel, Inc.). The slow axes of the microstructured and bow tie fibers were both oriented parallel to the surface of the composite panel. The orientation of the polarization axes has been checked afterward in cross sections of the composite coupon (Table I). The orientation for the bow tie and microstructured fiber are almost identical for the first sample, but differ for the second sample.

III. RESPONSE OF THE EMBEDDED FBGs UNDER VARIOUS LOADING CONDITIONS

Three different loading conditions were used to compare the response of the different sensors: a four-point bending test, a transversal load test, and a thermal test. The bending test is representative of an actual load condition on a structural component such as an airplane wing. The transversal load test allows comparing the transversal sensitivities for the different grating sensor technologies. Finally, a thermal test has been carried out to assess the differences in cross-sensitivity to temperature. For the mechanical experiments, the value of the applied load was measured with an electrical load cell. The Bragg peak wavelengths were recorded using an amplified spontaneous emission (ASE) source (nonflattened) and a commercial FBG interrogator (FBG-scan 600 from FOS&S) with a resolution of 1 pm and a repeatability better than 1 pm. Peak detection is based on a mean wavelength determination at −3 dB of the maximum peak power.

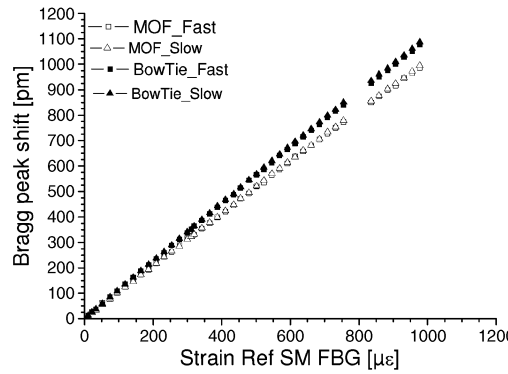

Fig. 2. Peak shifts measured during the four-point bending test for the different embedded FBGs versus the strain measured by the reference sensor for sample 1.

TABLE II
FBG SENSITIVITIES VERSUS AXIAL BENDING STRAIN OF THE COMPOSITE MATERIAL

	Sample 1[pm/με]	Sample 2[pm/με]
Bow tie slow axis	1.115	0.998
Bow tie fast axis	1.103	0.996
MOF slow axis	1.020	1.029
MOF fast axis	1.011	1.023

TABLE III
FBG SENSITIVITIES VERSUS TRANSVERSAL STRAIN OF THE COMPOSITE MATERIAL

	Sample 1 [pm/με]	Sample 2 [pm/με]
Bow tie slow axis	0.089	0.061
Bow tie fast axis	0.068	0.052
MOF slow axis	0.058	0.047
MOF fast axis	0.043	0.036
Bow tie peak separation	-0.022	-0.010
MOF peak separation	-0.014	-0.010

A. Four-Point Bending Test

The curves show similar slopes for both sensors (Fig. 2). The MOFs have the same orientation in both samples (Table I) and show equal sensitivities during bending (fitted values; see Table II). The orientation of the bow tie gratings, however, is different. The sensitivity of the less favorably oriented bow tie in sample 2 is approximately 10% lower than for the first sample. Where both bow tie and microstructured fiber have almost the same orientation in sample 1, the sensitivity is slightly different (approximately 8%).

B. Transversal Strain Test

The transversal strain response of the two grating types shows moderate differences (Table III). The transversal strain is derived from the applied transversal load and the material's transverse Young modulus of 6 GPa.

The transversal sensitivities of the FBG in the bow tie fiber are slightly higher. This difference can be partly attributed to the smaller cladding diameter of the bow tie fiber. For the Bragg peak separation, the sensitivities of the MOF FBG and the bow

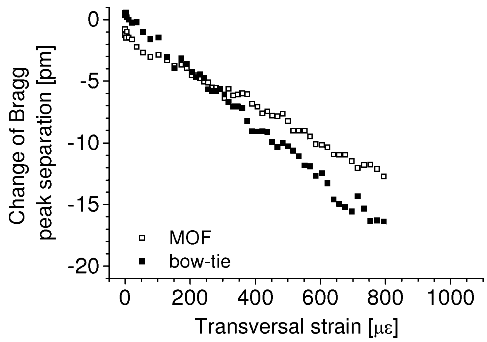

Fig. 3. Change of the peak separation versus transversally applied strain in the FBG for the MOF and bow tie fibers in sample 1.

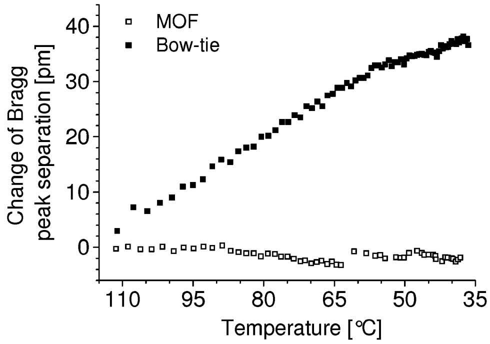

Fig. 4. Change of the peak separation in the FBG in the MOF and bow tie during the cooling down phase (sample 1).

tie FBG are in reasonable agreement (Fig. 3). The current differences between the MOF FBG and the bow tie FBG can be related to the different orientation of the polarization axes at the FBG location.

C. Temperature Test

For thermal cycling, the composite samples were heated up to 120 °C and were then allowed to cool down slowly in a climate chamber. During the cooling period, the peak wavelength separation was monitored. Fig. 4 shows that the linear change of the peak separation due to temperature is much smaller in the microstructured fiber (0.026 pm/°C) than in the bow tie fiber (−0.42 pm/°C). Since the phase modal birefringence in both fibers has a different origin, the thermal behavior of the Bragg peak wavelength separation differs. Indeed, the stress-induced material birefringence in a bow tie fiber is inherently temperature dependent, whereas the geometrical birefringence in the MOF is far less temperature sensitive and can even be zero at a particular wavelength [15]. We can, therefore, state that the Bragg peak separation in a highly birefringent microstructured fiber provides a quasi-temperature-independent measurement for the transversal strain in the composite material.

In addition, this measurement requires no absolute Bragg peak wavelength detection since it is based solely on the Bragg peak separation.

IV. Conclusion

The optical response of embedded FBGs written in the conventional bow tie fiber and birefringent MOF were compared for different loading conditions. Although the MOF, which was reported here, was not yet optimized to feature high axial or transversal strain sensitivities, our results show that such FBGs in MOF can already be an alternative to FBGs in conventional birefringent fibers. They both show similar response to mechanical loading, and in addition, the response to temperature changes shows important differences (bow tie FBG: −0.42 pm/°C, MOF FBG: 0.026 pm/°C), implying that the MOF FBG can operate almost independently of temperature variations.

We thus evidenced that microstructured fibers can be valuable components for structural integrity monitoring purposes in composite materials.

Acknowledgment

Ghent University acknowledges the European Space Agency for the material provided during the MASSFOS project and FOS&S for providing FBGs and the interrogation system.

References

[1] A. Othonos and K. Kalli, *Fiber Bragg Gratings: Fundamentals and Applications in Telecommunications and Sensing*. Boston, MA: Artech House, 1999.

[2] G. Luyckx *et al.*, "Three-dimensional strain and temperature monitoring of composite laminates," *Insight*, vol. 49, no. 1, pp. 10–16, 2007.

[3] E. Chehura, C. C. Ye, S. E. Staines, S. W. James, and R. P. Tatam, "Characterization of the response of fibre Bragg gratings fabricated in stress and geometrically induced high birefringence fibres to temperature and transverse load," *Smart Mater. Struct.*, vol. 13, pp. 888–895, 2004.

[4] I. Abe, O. Frazao, M. W. Schiller, R. N. Nogueira, H. J. Kalinowski, and J. L. Pinto, "Bragg gratings in normal and reduced diameter high birefringence fibre optics," *Meas. Sci. Technol.*, vol. 17, pp. 1477–1484, 2006.

[5] R. Montanini and L. D'Acquisto, "Simultaneous measurement of temperature and strain in glass fiber/epoxy composites by embedded fiber optic sensors: I cure monitoring," *Smart Mater. Struct.*, vol. 16, pp. 1718–1726, 2007.

[6] M. Mulle, R. Zitoune, F. Collombet, P. Olivier, and Y.-H. Grunevald, "Thermal expansion of carbon-epoxy laminates measured with embedded FBGS—Comparison with other experimental techniques and numerical simulation," *Composites Part A: Appl. Sci. Manuf.*, vol. 38, pp. 1414–1424, 2007.

[7] N. Tanaka, Y. Okabel, and N. Takeda, "Temperature-compensated strain measurement using fiber Bragg grating sensors embedded in composites laminates," *Smart mater. Struct.*, vol. 12, no. 12, pp. 940–946, 2003.

[8] P. St. J. Russell, "Photonic-crystal fibers," *J. Lightw. Technol.*, vol. 24, no. 12, pp. 4729–4749, Dec. 2006.

[9] B. J. Eggleton, P. S. Westbrook, R. S. Windeler, S. Spalter, and T. A. Strasser, "Grating resonances in air-silica microstructured optical fibers," *Opt. Lett.*, vol. 24, no. 21, pp. 1460–1462, 1999.

[10] V. Beugin *et al.*, "Efficient Bragg gratings in phosphosilicate and germanosilicate photonic crystal fiber," *Appl. Opt.*, vol. 45, pp. 8186–8193, 2006.

[11] T. Geernaert *et al.*, "Fiber Bragg gratings in germanium-doped highly birefringent microstructured optical fibers," *IEEE Photon. Technol. Lett.*, vol. 20, no. 8, pp. 554–556, Apr. 2008.

[12] J. Canning, N. Groothoff, and K. Cook *et al.*, "Gratings in structured optical fibres," *Laser Chem.*, vol. 2008, pp. 239417-1–239417-19, 2008.

[13] Y. Wang *et al.*, "Sensing properties of fiber Bragg gratings in small-core Ge-doped photonic crystal fibers," *Opt. Commun.*, vol. 282, pp. 1129–1134, 2009.

[14] T. Geernaert *et al.*, "Transversal load sensing with Fiber Bragg gratings in microstructured optical fibers," *IEEE Photon. Technol. Lett.*, vol. 21, no. 1, pp. 6–8, Jan. 1, 2009.

[15] T. Martynkien, M. Szpulak, and W. Urbanczyk, "Modeling and measurement of temperature sensitivity in birefringent photonic crystal holey fibers," *Appl. Opt.*, vol. 44, pp. 7780–7788, 2005.